Acta Cryst E CRYSTALLOGRAPHIC COMMUNICATIONS

ISSN 2056-9890

Crystal structure and Hirshfeld surface analysis of $[FeCl_4(LH)_2]$ (*L*H = 1*H*-imidazo[4,5-*b*]pyridin-4-ium)

Soffa Imene,[a] Bouhidel Zakaria,[a] Sahli Kaouther,[b] Cherouana Aouatef[a]* and Bendeif El-Eulmi[c,d]

[a]Unité de Recherche de Chimie de l'Environnement et Moléculaire Structurale (URCHEMS), Département de Chimie, Université Mentouri de Constantine, 25000 Constantine, Algeria, [b]Pharmaceutical Sciences Research Center CRSP, Constantine 25000, Algeria, [c]Synchrotron SOLEIL, L'Orme des Merisiers, BP48, Saint Aubin, 91192, Gif-sur-Yvette, France, and [d]Laboratoire de Cristallographie, Résonance Magnétique et Modélisation CRM2, UMR 7036, Institut Jean Barriol Faculté des Sciences et Technologies, BP 70239, 54506 Vandoeuvre lès Nancy, France. *Correspondence e-mail: cherouana.aouatef@umc.edu.dz

Received 31 July 2025
Accepted 26 November 2025

Edited by F. Di Salvo, University of Buenos Aires, Argentina

Keywords: 4-azabenzimidazole; iron; crystal structure; Hirshfeld surface analysis.

CCDC reference: 2505852

Supporting information: this article has supporting information at journals.iucr.org/e

The title coordination complex tetrachloridobis(1*H*-imidazo[4,5-*b*]pyridin-4-ium-κN^3)iron(II), $[FeCl_4(C_6H_6N_3)_2]$ or $[FeCl_4(LH)_2]$, was synthesized and structurally characterized by single-crystal X-ray diffraction. The complex crystallizes in the triclinic space group $P\overline{1}$. The iron atom (site symmetry $\overline{1}$) is hexa-coordinated, adopting a slightly distorted octahedral geometry defined by two 1*H*-imidazo[4,5-*b*]pyridinium ligands and four chloride anions. In the crystal, N—H···Cl hydrogen bonds generate two-dimensional layers parallel to the *ab* plane, while the three-dimensional supramolecular framework is further consolidated by C—H···Cl interactions. In addition, π–π stacking interactions contribute to the overall cohesion of the crystal structure. Hirshfeld surface analysis indicates the significance of various intermolecular contacts in the crystal packing, with major contributions from Cl···H/H···Cl (43.2%), H···H (22.5%), C···H/H···C (16.4%), H···N/N···H (4.4%), N···C/C···N (3.7%), C···C (3.6%), Cl···N/N···Cl (3.2%), Cl···C/C···Cl (2.4%), and N···N (0.6%) interactions.

1. Chemical context

The coordination chemistry of iron has attracted great interest due to the importance of iron-based coordination compounds and their applications in various fields such as catalysis (Sheldon & Kochi, 1981; Meunier *et al.*, 2000), magnetism (Toftlund, 1989; Gütlich, 1981) and bioinorganic chemistry, particularly in simulating the behaviour of enzymes involved in electron transfer and oxygen transfer processes (Reedijk & Bouwman, 1999). Iron is frequently hexacoordinated in its coordination complexes; it is important to note that the number, type, and geometric arrangement of ligands around the metal centre significantly influence the previously mentioned properties (Börzel *et al.*, 2002).

Nitrogen-containing heterocycles, which feature one or more nitrogen atoms within their ring structures, represent important and distinctive categories of heterocycles (Li *et al.*, 2023). These heterocycles play an important role in coordination chemistry as N-donor ligands. Among them, benzimidazole is particularly well known and widely used as a nitrogen-donor ligand (Ana, 2019).

Benzimidazole contains two N-donor atoms that can coordinate transition metals (Sundberg & Martin, 1974). The imidazole ring consists of two nitrogen atoms, one of which is pyrrole-like, with its lone pair electrons contributing to the

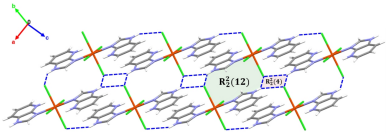

aromatic sextet. The second N atom is pyridine-like, with a non-delocalized lone pair that imparts basic properties (Haga, 2003). The substitution of a CH group in the benzene ring with a nitrogen atom, which is necessarily pyridine-like, imparts a basicity similar to that of nitrogen in the imidazole ring. This modification enhances the ligand's basic properties by introducing a second pyridine-like nitrogen atom, thereby increasing its binding affinity to metal ions (Zapata *et al.*, 2008). Thus, 4-azabenzimidazole consists of a fused imidazole and pyridine system. The positioning of its basic nitrogen atoms enables the potential for chelation with metal ions, facilitating the formation of four-membered rings (Korabik *et al.*, 1998). The three nitrogen atoms in 4-azabenzimidazole, each with distinct characteristics, provide versatility to the ligand, allowing it to coordinate with metal ions in various modes, including monodentate, bidentate, chelating, and bridging arrangements.

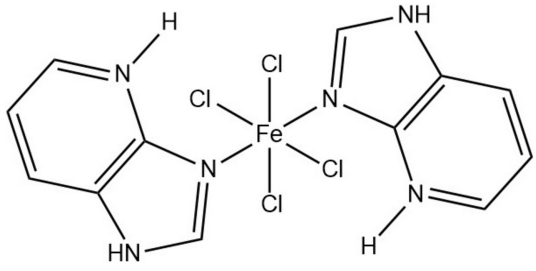

2. Structural commentary

The title complex crystallizes with the Fe^{2+} atom located on a crystallographic centre of symmetry, generating the complete molecule by inversion symmetry. As a result, the structure consists of two symmetry-related halves forming a discrete mononuclear complex with an octahedral geometry and a trans configuration for the N atoms. The Fe^{2+} centre is coordinated by two nitrogen atoms from two N-donor 1*H*-imidazo[4,5-*b*]pyridinium ligands in the axial positions and four chloride ions in the equatorial plane (Fig. 1), resulting in an N_2Cl_4 coordination environment. The bond lengths and angles (Table 1) are consistent with a slightly distorted octahedral geometry. The axial Fe1—N1 bond length is 2.2256 (9) Å, whereas the equatorial Fe1—Cl1 and Fe1—Cl2 bond lengths

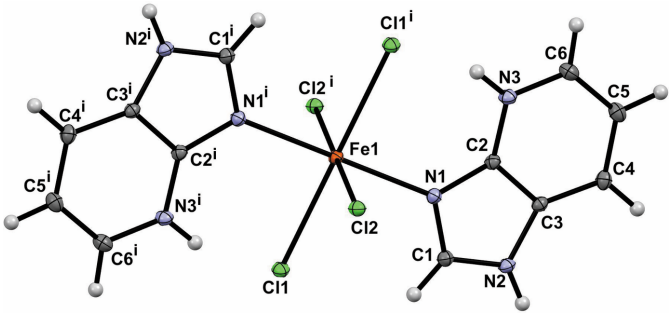

Figure 1
ORTEP view of the structure of the title complex showing the atom-labelling scheme. Displacement ellipsoids are drawn at the 50% probability level. Symmetry code: (i) $-x, -y, -z$.

Table 1
Selected geometric parameters (Å, °).

Fe1—Cl1	2.5845 (2)	Fe1—N1	2.2256 (9)
Fe1—Cl2	2.4564 (2)		
Cl1—Fe1—Cl2	89.75 (1)	Cl1—Fe1—N1^{i}	92.41 (2)
Cl1—Fe1—N1	87.59 (2)	Cl2—Fe1—N1	92.50 (2)
Cl1—Fe1—Cl2^{i}	90.25 (1)	Cl2—Fe1—N1^{i}	87.50 (2)

Symmetry code: (i) $-x, -y, -z$.

Table 2
Hydrogen-bond geometry (Å, °).

D—H···A	D—H	H···A	D···A	D—H···A
N2—H2···Cl2^{ii}	0.86 (2)	2.66 (2)	3.3061 (10)	133.0 (17)
N2—H2···Cl2^{iii}	0.86 (2)	2.56 (2)	3.1862 (9)	130.4 (17)
N3—H3···Cl1^{i}	0.89 (2)	2.15 (2)	2.9944 (10)	160.7 (19)
C1—H1···Cl1	0.942 (15)	2.702 (15)	3.2841 (10)	120.7 (11)
C5—H5···Cl2^{iv}	0.958 (15)	2.725 (15)	3.6357 (10)	159.1 (12)
C6—H6···Cl1^{v}	0.954 (15)	2.641 (15)	3.5932 (11)	176.2 (13)

Symmetry codes: (i) $-x, -y, -z$; (ii) $x+1, y+1, z$; (iii) $-x+1, -y, -z$; (iv) $-x+1, -y+1, -z+1$; (v) $x, y+1, z+1$.

are 2.5845 (2) and 2.4564 (2) Å, respectively. These values fall within the expected range for Fe^{2+} octahedral complexes reported in the literature (Rettig *et al.*, 2000; Rusbridge *et al.*, 2018). The bond angles around the metal centre are close to the ideal values of 90°, with only minor deviations, confirming a near-ideal octahedral coordination geometry. Moreover, the iron(II) atom lies within the equatorial plane, while the five-membered imidazole and six-membered pyridine rings of the chelating ligand are approximately coplanar, allowing for efficient coordination and contributing to the overall planarity of the ligand framework. The cohesion of the molecular structure is achieved through an intramolecular N—H···Cl hydrogen bond formed between the nitrogen atom of the imidazole ring and a chloride ion acceptor [N3—H3···Cl1^{i}; symmetry code: (i) $-x, -y, -z$).

3. Supramolecular features

The crystal structure of the title compound is consolidated by various supramolecular interactions, including classical and non-classical hydrogen bonds, as well as π–π stacking interactions. All N—H and C—H groups of the 1*H*-imidazo[4,5-*b*]pyridinium ligand, except for the C4—H4 group, act as hydrogen-bond donors, while the chloride ions serve as acceptors, forming N—H···Cl and C—H···Cl interactions (Table 2). Furthermore, N2—H2···Cl2^{ii} hydrogen bonding

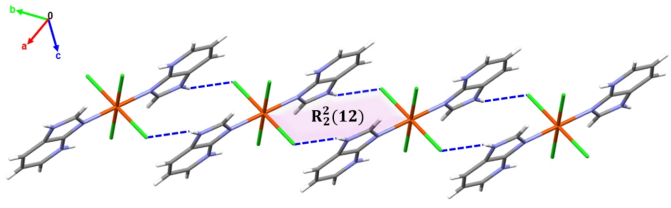

Figure 2
Network propagation along the [110] direction through N2—H2···Cl2^{ii} hydrogen bonds, forming $R_2^2(12)$ graph-set motifs (highlighted in purple).

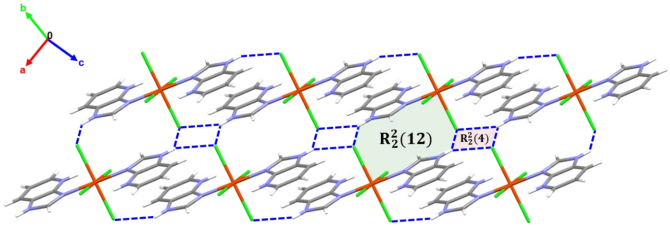

Figure 3
Two-dimensional network of the title compound parallel to the *ab* plane, showing N—H···Cl hydrogen bonds and associated ring motifs.

links the molecules into chains along the [110] direction. These chains adopt a ribbon-like arrangement featuring $R_2^2(12)$ ring motifs (Fig. 2; Bernstein *et al.*, 1995). These chains are further connected *via* classical hydrogen bonds (N2—H2···Cl2^{iii}) into a two-dimensional network lying parallel to the (001) plane, based on alternating $R_2^2(4)$ and $R_2^2(12)$ ring motifs (Fig. 3). Extension into a three-dimensional network occurs *via* non-classical C—H···Cl hydrogen bonds C5—H5···Cl2^{v} and C6—H6···Cl1^{iv}, forming $R_2^2(14)$, $R_2^4(14)$ and $R_2^3(11)$ graph-set motifs (Fig. 4).

Overall, the crystal packing is reinforced by π–π stacking interactions involving both the six-membered pyridine rings (*Cg*6) and the five-membered imidazole rings (*Cg*5) of neighbouring molecules in a parallel-displaced arrangement (Fig. 5) with centroid–centroid distances of 3.591 (1) and 3.459 (1) Å, respectively

To gain a deeper insight into the intermolecular interactions responsible for the cohesion and stability of the supramolecular structure, a Hirshfeld surface (HS) analysis was performed using *Crystal Explorer 21* (Spackman & Jayatilaka, 2009; Spackman *et al.*, 2021). The two-dimensional fingerprint plots (Fig. 6; Spackman & McKinnon, 2002) show that Cl···H/H···Cl contacts are the most significant (43.2%), followed by H···H (22.5%) and C···H/H···C (16.4%). Minor contributions arise from H···N/N···H (4.4%), C···N/N···C (3.7%), C···C (3.6%), and Cl···N/N···Cl (3.2%), while Cl···C/C···Cl (2.4%) and N···N (0.6%) are negligible. Overall, the HS analysis emphasizes the role of hydrogen bonding and van der Waals interactions (Hökelek *et al.*, 2018; Hathwar *et al.*, 2015) in consolidating the packing, together with π–π stacking. In addition, it confirms the absence of halogen–halogen contacts, as the Cl···Cl contribution is 0% (Moon *et al.*, 2020).

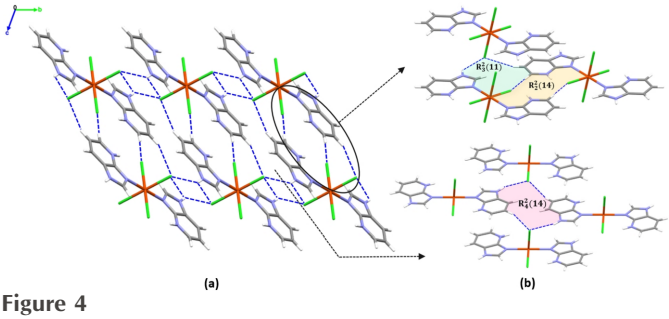

Figure 4
(*a*) Fragment of the supramolecular crystal structure packing of the title compound, (*b*) hydrogen-bonding patterns. Hydrogen bonds are indicated by dashed blue lines.

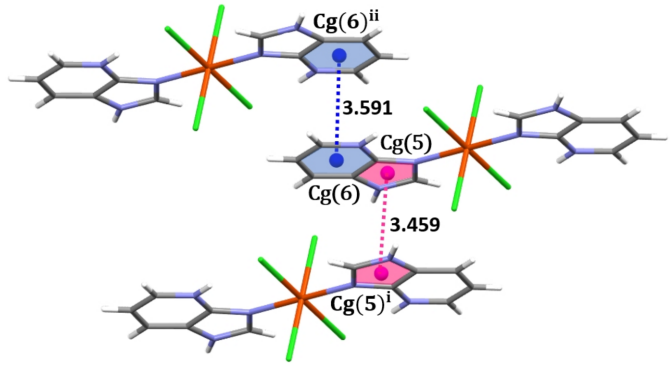

Figure 5
π–π stacking interactions in the title complex. *Cg*(5) and *Cg*(6) are the centroids of imidazole rings (pink) and pyridine rings (blue), respectively, [symmetry codes: (i) $1-x, 1-y, 1-z$; (ii) $1-x, 1-y, -z$].

4. Database survey

A Cambridge Structural Database (CSD, version 5.45, November 2023 update; Groom *et al.*, 2016; Bruno *et al.*, 2002) search revealed only one reported iron complex with 4-azabenzimidazole, where the ligand acts in a bridging mode *via* the two imidazole N atoms generating a three-dimensional diamond-like framework (refcode XASGON; Rettig *et al.*, 2000). A zinc analogue with the same coordination mode has also been described (MIHHOB; Hayashi *et al.*, 2007).

In contrast, several copper complexes display diverse coordination behaviours. In some cases, the ligand coordinates in a monodentate fashion via the amine nitrogen [GEZCOF (Domínguez-Martín *et al.*, 2013); BUNZEQ (Choquesillo-Lazarte *et al.*, 2010)], while in others, coordination occurs through the imine nitrogen, as in the title compound (GEZCIZ; Domínguez-Martín *et al.*, 2013). Alternatively, 4-azabenzimidazole can act as a bridging ligand through both the imine and pyridinic nitrogen atoms, affording dinuclear Cu^{II} paddlewheel-like architectures (TETGIJ and TETGOP; van Albada *et al.*, 2006).

To date, no structures have been reported with 4-azabenzimidazole protonated at the pyridinic nitrogen atom, until the present compound.

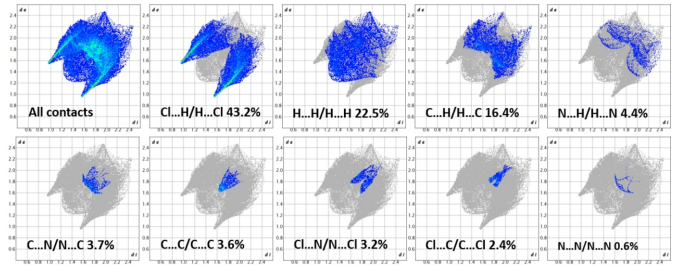

Figure 6
Two-dimensional fingerprint plots for the title compound with the corresponding Hirshfeld surface d_{norm} for all contacts and those delineated into specific contacts. The d_i and d_e values represent the nearest internal and external distances from specific points on the Hirshfeld surface (in Å).

5. Experimental

All chemicals were commercially available, purchased from Sigma-Aldrich, and used as received without purification.

5.1. Synthesis and crystallization

$FeCl_2{\cdot}4H_2O$ (0.198 g, 1 mmol) was dissolved in 10 mL of methanol in the presence of a few drops of ascorbic acid. A solution of 4-azabenzimidazole (0.238 g, 2 mmol) in 10 mL of acetonitrile was then added, resulting in a brown mixture, which was heated under stirring until boiling. The solution was left to evaporate slowly over several days, yielding green crystals of the title compound, suitable for single-crystal X-ray diffraction analysis.

5.2. Refinement

Crystal data, data collection and structure refinement details are summarized in Table 3. All hydrogen atoms were located from difference Fourier maps and refined freely with isotropic displacement parameters.

Table 3
Experimental details.

Crystal data	
Chemical formula	$[FeCl_4(C_6H_6N_3)_2]$
M_r	437.93
Crystal system, space group	Triclinic, $P\overline{1}$
Temperature (K)	100
a, b, c (Å)	6.9242 (2), 7.5223 (2), 8.6704 (2)
α, β, γ (°)	106.967 (2), 98.665 (2), 109.174 (2)
V (Å^3)	392.51 (1)
Z	1
Radiation type	Mo $K\alpha$
μ (mm^{-1})	1.65
Crystal size (mm)	0.10 × 0.09 × 0.08
Data collection	
Diffractometer	Nonius KappaCCD
No. of measured, independent and observed [$I > 2\sigma(I)$] reflections	30304, 2818, 2650
R_{int}	0.026
$(\sin\theta/\lambda)_{max}$ (Å^{-1})	0.764
Refinement	
$R[F^2 > 2\sigma(F^2)]$, $wR(F^2)$, S	0.019, 0.049, 1.07
No. of reflections	2818
No. of parameters	130
H-atom treatment	All H-atom parameters refined
$\Delta\rho_{max}$, $\Delta\rho_{min}$ (e Å^{-3})	0.51, −0.27

Computer programs: *APEX2* and *SAINT* (Bruker, 2024), *SHELXT* (Sheldrick, 2015*a*), *SHELXL2018/3* (Sheldrick, 2015*b*) and *OLEX2* (Dolomanov *et al.*, 2009).

Acknowledgements

The authors acknowledge the Algerian Ministry of Higher Education and Scientific Research, the Algerian Directorate-General for Scientific Research and Technological Development for support.

References

Ana, B. (2019). *Chemistry and Applications of Benzimidazole and its Derivatives* edited by M. Maria, ch. 11. Rijeka: IntechOpen. https://doi. org/10.5772/intechopen. 85333
Bernstein, J., Davis, R. E., Shimoni, L. & Chang, N.-L. (1995). *Angew. Chem. Int. Ed. Engl.* **34**, 1555–1573.
Börzel, H., Comba, P., Hagen, K. S., Lampeka, Y. D., Lienke, A., Linti, G., Merz, M., Pritzkow, H. & Tsymbal, L. V. (2002). *Inorg. Chim. Acta* **337**, 407–419.
Bruker (2024). *APEX2* and *SAINT*. Bruker AXS Inc., Madison, Wisconsin, USA.
Bruno, I. J., Cole, J. C., Edgington, P. R., Kessler, M., Macrae, C. F., McCabe, P., Pearson, J. & Taylor, R. (2002). *Acta Cryst.* B**58**, 389–397.
Choquesillo-Lazarte, D., Domínguez-Martín, A., Matilla-Hernández, A., Sánchez de Medina-Revilla, C., González-Pérez, J. M., Castiñeiras, A. & Niclós-Gutiérrez, J. (2010). *Polyhedron* **29**, 170–177.
Dolomanov, O. V., Bourhis, L. J., Gildea, R. J., Howard, J. A. K. & Puschmann, H. (2009). *J. Appl. Cryst.* **42**, 339–341.
Domínguez-Martín, A., Choquesillo-Lazarte, D., Dobado, J. A., Vidal, I., Lezama, L., González-Pérez, J. M., Castiñeiras, A. & Niclós-Gutiérrez, J. (2013). *Dalton Trans.* **42**, 6119–6130.
Groom, C. R., Bruno, I. J., Lightfoot, M. P. & Ward, S. C. (2016). *Acta Cryst.* B**72**, 171–179.
Gütlich, P. (1981). *Metal Complexes* edited by R. Bau, P. Gütlich & R. G. Teller, pp. 83–195. Berlin, Heidelberg: Springer. https://doi. org/10.1007/BFb0111269
Haga, M. (2003). *Comprehensive Coordination Chemistry II* edited by J. A. McCleverty & T. J. Meyer, pp. 125-134. Oxford: Pergamon. https://doi. org/10.1016/B0-08-043748-6/01095-1
Hathwar, V. R., Sist, M., Jørgensen, M. R. V., Mamakhel, A. H., Wang, X., Hoffmann, C. M., Sugimoto, K., Overgaard, J. & Iversen, B. B. (2015). *IUCrJ* **2**, 563–574.
Hayashi, H., Côté, A. P., Furukawa, H., O'Keeffe, M. & Yaghi, O. M. (2007). *Nat. Mater.* **6**, 501–506.
Hökelek, T., Yavuz, V., Dal, H. & Necefoğlu, H. (2018). *Acta Cryst.* E**74**, 45–50.
Korabik, M., Materny, M., Surga, W., Głowiak, T. & Mroziński, J. (1998). *J. Mol. Struct.* **443**, 255–263.
Li, Y., Liu, T. & Sun, J. (2023). *Molecules* **28**, 733.
Meunier, B., Brudvig, G., McLain, J. L., Murahashi, S., **-i**, Pecoraro, V., Riley, D., Robert, A., Rodriguez, J., Sheldon, R. & Valentine, J. (2000). *Biomimetic Oxidations Catalyzed by Transition Metal Complexes*. Singapore: World Scientific. https://doi. org/10.1142/p084.
Moon, D., Jeon, J. & Choi, J.-H. (2020). *J. Coord. Chem.* **73**, 2029–2041.
Reedijk, J. & Bouwman, E. (1999). *Bioinorganic Catalysis*. Boca Raton, FL: CRC Press. https://doi. org/10.1201/9780203908457.
Rettig, S. J., Sánchez, V., Storr, A., Thompson, R. C. & Trotter, J. (2000). *J. Chem. Soc. Dalton Trans.* pp. 3931–3937.
Rusbridge, E. K., Peng, Y., Powell, A. K., Robinson, D. & Fitzpatrick, A. J. (2018). *Dalton Trans.* **47**, 7644–7648.
Sheldon, R. A. & Kochi, J. K. (1981). *Metal-Catalyzed Oxidations of Organic Compounds*. New York: Academic Press. https://doi. org/10.1016/B978-0-12-639380-4.X5001-5.
Sheldrick, G. M. (2015*a*). *Acta Cryst.* A**71**, 3–8.
Sheldrick, G. M. (2015*b*). *Acta Cryst.* C**71**, 3–8.
Spackman, M. A. & Jayatilaka, D. (2009). *CrystEngComm* **11**, 19–32.
Spackman, M. A. & McKinnon, J. J. (2002). *CrystEngComm* **4**, 378–392.
Spackman, P. R., Turner, M. J., McKinnon, J. J., Wolff, S. K., Grimwood, D. J., Jayatilaka, D. & Spackman, M. A. (2021). *J. Appl. Cryst.* **54**, 1006–1011.
Sundberg, R. J. & Martin, R. B. (1974). *Chem. Rev.* **74**, 471–517.
Toftlund, H. (1989). *Coord. Chem. Rev.* **94**, 67–108.
van Albada, G. A., Mutikainen, I., Turpeinen, U. & Reedijk, J. (2006). *Polyhedron* **25**, 3278–3284.
Zapata, F., Caballero, A., Espinosa, A., Tárraga, A. & Molina, P. (2008). *Org. Lett.* **10**, 41–44.

supporting information

Acta Cryst. (2026). E**82**, 10-13 [https://doi.org/10.1107/S2056989025010564]

Crystal structure and Hirshfeld surface analysis of $[FeCl_4(\mathit{L}H)_2]$ ($\mathit{L}H$ = 1*H*-imidazo[4,5-*b*]pyridin-4-ium)

Soffa Imene, Bouhidel Zakaria, Sahli Kaouther, Cherouana Aouatef and Bendeif El-Eulmi

Computing details

Tetrachloridobis(1*H*-imidazo[4,5-*b*]pyridin-4-ium-κN^3)iron(II)

Crystal data

$[FeCl_4(C_6H_6N_3)_2]$
M_r = 437.93
Triclinic, $P\overline{1}$
Hall symbol: -P 1
a = 6.9242 (2) Å
b = 7.5223 (2) Å
c = 8.6704 (2) Å
α = 106.967 (2)°
β = 98.665 (2)°
γ = 109.174 (2)°
V = 392.51 (1) Å^3
Z = 1
$F(000)$ = 220
D_x = 1.853 Mg m^{-3}
Mo $K\alpha$ radiation, λ = 0.71073 Å
Cell parameters from 30213 reflections
θ = 3.1–32.9°
μ = 1.65 mm^{-1}
T = 100 K
Prism, green
0.1 × 0.09 × 0.08 mm

Data collection

Nonius KappaCCD diffractometer
Radiation source: fine-focus sealed tube
ω scans
30304 measured reflections
2818 independent reflections
2650 reflections with $I > 2\sigma(I)$
R_{int} = 0.026
θ_{max} = 32.9°, θ_{min} = 3.1°
h = −10→10
k = −11→11
l = −12→13

Refinement

Refinement on F^2
Least-squares matrix: full
$R[F^2 > 2\sigma(F^2)]$ = 0.019
$wR(F^2)$ = 0.049
S = 1.07
2818 reflections
130 parameters
0 restraints
Hydrogen site location: difference Fourier map
All H-atom parameters refined
$w = 1/[\sigma^2(F_o^2) + (0.0225P)^2 + 0.1909P]$ where $P = (F_o^2 + 2F_c^2)/3$
$(\Delta/\sigma)_{max}$ = 0.001
$\Delta\rho_{max}$ = 0.51 e Å^{-3}
$\Delta\rho_{min}$ = −0.26 e Å^{-3}

Special details

Geometry. Bond distances, angles etc. have been calculated using the rounded fractional coordinates. All su's are estimated from the variances of the (full) variance-covariance matrix. The cell esds are taken into account in the estimation of distances, angles and torsion angles

Fractional atomic coordinates and isotropic or equivalent isotropic displacement parameters (Å²)

	x	*y*	*z*	U_{iso}*/U_{eq}
Fe1	0.00000	0.00000	0.00000	0.0091 (1)
Cl1	0.11270 (3)	−0.15421 (3)	−0.26126 (3)	0.0118 (1)
Cl2	0.10569 (3)	−0.21585 (3)	0.12967 (3)	0.0112 (1)
N1	0.32581 (13)	0.24252 (12)	0.09987 (10)	0.0104 (2)
N2	0.65992 (13)	0.42459 (12)	0.10840 (10)	0.0110 (2)
N3	0.30049 (13)	0.49999 (12)	0.33328 (10)	0.0116 (2)
C1	0.48880 (15)	0.24861 (14)	0.03344 (12)	0.0112 (2)
C2	0.40177 (14)	0.42778 (13)	0.22624 (11)	0.0096 (2)
C3	0.61149 (14)	0.54528 (14)	0.23671 (11)	0.0101 (2)
C4	0.72138 (15)	0.73656 (14)	0.35954 (12)	0.0127 (2)
C5	0.61028 (16)	0.80452 (15)	0.46871 (12)	0.0142 (2)
C6	0.40167 (16)	0.68616 (15)	0.45319 (12)	0.0136 (2)
H1	0.486 (2)	0.141 (2)	−0.0572 (18)	0.014 (3)*
H2	0.779 (3)	0.447 (3)	0.084 (2)	0.025 (4)*
H3	0.169 (3)	0.421 (3)	0.324 (2)	0.028 (4)*
H4	0.867 (2)	0.817 (2)	0.3706 (19)	0.018 (4)*
H5	0.676 (2)	0.934 (2)	0.5580 (19)	0.019 (4)*
H6	0.320 (2)	0.728 (2)	0.5245 (19)	0.018 (3)*

Atomic displacement parameters (Å²)

	U^{11}	U^{22}	U^{33}	U^{12}	U^{13}	U^{23}
Fe1	0.0081 (1)	0.0083 (1)	0.0104 (1)	0.0026 (1)	0.0036 (1)	0.0031 (1)
Cl1	0.0110 (1)	0.0115 (1)	0.0125 (1)	0.0038 (1)	0.0055 (1)	0.0035 (1)
Cl2	0.0110 (1)	0.0109 (1)	0.0127 (1)	0.0049 (1)	0.0048 (1)	0.0043 (1)
N1	0.0098 (3)	0.0095 (3)	0.0113 (3)	0.0034 (3)	0.0035 (3)	0.0030 (3)
N2	0.0089 (3)	0.0120 (3)	0.0127 (3)	0.0042 (3)	0.0048 (3)	0.0044 (3)
N3	0.0112 (3)	0.0114 (3)	0.0131 (3)	0.0043 (3)	0.0058 (3)	0.0047 (3)
C1	0.0105 (4)	0.0112 (4)	0.0121 (4)	0.0045 (3)	0.0037 (3)	0.0038 (3)
C2	0.0092 (4)	0.0092 (4)	0.0108 (3)	0.0033 (3)	0.0034 (3)	0.0042 (3)
C3	0.0095 (4)	0.0109 (4)	0.0106 (4)	0.0040 (3)	0.0033 (3)	0.0047 (3)
C4	0.0117 (4)	0.0112 (4)	0.0131 (4)	0.0022 (3)	0.0023 (3)	0.0046 (3)
C5	0.0161 (4)	0.0109 (4)	0.0133 (4)	0.0041 (3)	0.0033 (3)	0.0030 (3)
C6	0.0166 (4)	0.0125 (4)	0.0127 (4)	0.0069 (3)	0.0058 (3)	0.0036 (3)

Geometric parameters (Å, º)

Fe1—Cl1	2.5845 (2)	N3—C6	1.3488 (14)
Fe1—Cl2	2.4564 (2)	C2—C3	1.4030 (15)
Fe1—N1	2.2256 (9)	N2—H2	0.86 (2)
Fe1—Cl1^{i}	2.5845 (2)	N3—H3	0.89 (2)
Fe1—Cl2^{i}	2.4564 (2)	C3—C4	1.3877 (14)
Fe1—N1^{i}	2.2256 (9)	C4—C5	1.3944 (15)
N1—C1	1.3360 (14)	C5—C6	1.3871 (16)
N1—C2	1.3686 (13)	C1—H1	0.942 (15)

N2—C1	1.3469 (14)	C4—H4	0.964 (15)
N2—C3	1.3774 (13)	C5—H5	0.958 (15)
N3—C2	1.3418 (13)	C6—H6	0.954 (15)

Cl1—Fe1—Cl2	89.75 (1)	N1—C2—N3	127.71 (9)
Cl1—Fe1—N1	87.59 (2)	N1—C2—C3	111.74 (9)
Cl1—Fe1—Cl1^{i}	180.00	N3—C2—C3	120.54 (9)
Cl1—Fe1—Cl2^{i}	90.25 (1)	C3—N2—H2	128.4 (13)
Cl1—Fe1—N1^{i}	92.41 (2)	C1—N2—H2	124.0 (13)
Cl2—Fe1—N1	92.50 (2)	N2—C3—C4	134.70 (10)
Cl1^{i}—Fe1—Cl2	90.25 (1)	C2—C3—C4	121.25 (9)
Cl2—Fe1—Cl2^{i}	180.00	N2—C3—C2	104.04 (8)
Cl2—Fe1—N1^{i}	87.50 (2)	C2—N3—H3	118.1 (12)
Cl1^{i}—Fe1—N1	92.41 (2)	C6—N3—H3	122.1 (12)
Cl2^{i}—Fe1—N1	87.50 (2)	C3—C4—C5	116.15 (10)
N1—Fe1—N1^{i}	180.00	C4—C5—C6	121.22 (10)
Cl1^{i}—Fe1—Cl2^{i}	89.75 (1)	N3—C6—C5	121.01 (10)
Cl1^{i}—Fe1—N1^{i}	87.59 (2)	N1—C1—H1	123.8 (9)
Cl2^{i}—Fe1—N1^{i}	92.50 (2)	N2—C1—H1	122.6 (9)
Fe1—N1—C1	126.40 (7)	C3—C4—H4	122.1 (9)
Fe1—N1—C2	129.89 (7)	C5—C4—H4	121.7 (9)
C1—N1—C2	103.25 (9)	C4—C5—H5	121.1 (9)
C1—N2—C3	107.32 (9)	C6—C5—H5	117.6 (9)
C2—N3—C6	119.81 (9)	N3—C6—H6	115.3 (9)
N1—C1—N2	113.63 (9)	C5—C6—H6	123.7 (9)

Cl1—Fe1—N1—C1	−7.58 (8)	C3—N2—C1—N1	1.16 (12)
Cl1—Fe1—N1—C2	163.34 (8)	C1—N2—C3—C2	−1.28 (11)
Cl2—Fe1—N1—C1	82.07 (8)	C1—N2—C3—C4	177.73 (11)
Cl2—Fe1—N1—C2	−107.02 (8)	C6—N3—C2—N1	178.75 (10)
Cl1^{i}—Fe1—N1—C1	172.42 (8)	C6—N3—C2—C3	−0.74 (14)
Cl1^{i}—Fe1—N1—C2	−16.66 (8)	C2—N3—C6—C5	−0.45 (15)
Cl2^{i}—Fe1—N1—C1	−97.93 (8)	N1—C2—C3—N2	1.06 (11)
Cl2^{i}—Fe1—N1—C2	72.98 (8)	N1—C2—C3—C4	−178.12 (9)
Fe1—N1—C1—N2	172.38 (7)	N3—C2—C3—N2	−179.38 (9)
C2—N1—C1—N2	−0.47 (11)	N3—C2—C3—C4	1.45 (15)
Fe1—N1—C2—N3	7.58 (15)	N2—C3—C4—C5	−179.78 (11)
Fe1—N1—C2—C3	−172.89 (7)	C2—C3—C4—C5	−0.90 (15)
C1—N1—C2—N3	−179.92 (10)	C3—C4—C5—C6	−0.28 (15)
C1—N1—C2—C3	−0.39 (11)	C4—C5—C6—N3	0.98 (16)

Symmetry code: (i) −*x*, −*y*, −*z*.

Hydrogen-bond geometry (Å, º)

D—H···*A*	*D*—H	H···*A*	*D*···*A*	*D*—H···*A*
N2—H2···Cl2^{ii}	0.86 (2)	2.66 (2)	3.3061 (10)	133.0 (17)
N2—H2···Cl2^{iii}	0.86 (2)	2.56 (2)	3.1862 (9)	130.4 (17)

N3—H3···Cl1^{i}	0.89 (2)	2.15 (2)	2.9944 (10)	160.7 (19)
C1—H1···Cl1	0.942 (15)	2.702 (15)	3.2841 (10)	120.7 (11)
C5—H5···Cl2^{iv}	0.958 (15)	2.725 (15)	3.6357 (10)	159.1 (12)
C6—H6···Cl1^{v}	0.954 (15)	2.641 (15)	3.5932 (11)	176.2 (13)

Symmetry codes: (i) −*x*, −*y*, −*z*; (ii) *x*+1, *y*+1, *z*; (iii) −*x*+1, −*y*, −*z*; (iv) −*x*+1, −*y*+1, −*z*+1; (v) *x*, *y*+1, *z*+1.

Geometric parameters of π··· π stacking (Å, °)

Cg ⋯ Cg (Ring)	Cg ⋯ Cg (Å)	*α*(°)	*β*(°)	*γ*(°)
Cg(5) ⋯ Cg(5)i	3.459 (1)	0.00	23.13	23.13
Cg(6) ⋯ Cg(6)ii	3.591 (1)	0.00	21.67	21.67

Symmetry codes: (i) 1-x,1-y,-z, (ii) 1-x,1-y,1-z Cg(5): center of gravity of imidazole ring. Cg(6): center of gravity of pyridine ring. *α*: dihedral angle between ring planes. *β*, *γ*: Slipping angles defined by centroid–centroid vector and the normal to the plane of the ring.